


Bionanocomposites based on a covalent network of chitosan and edge functionalized graphene layers

Vincenzina Barbera¹ , Giulio Torrisi
and Maurizio Galimberti

Journal of Applied Biomaterials &
Functional Materials
Volume 19: 1–11
© The Author(s) 2021
Article reuse guidelines:
sagepub.com/journals-permissions
DOI: 10.1177/22808000211017431
journals.sagepub.com/home/jbf


Abstract

In this study, carbon papers and aerogels were prepared from chitosan and graphene layers with aldehydic edge functional groups (G-CHO) able to form chemical bonds with chitosan and thus to form a crosslinked network. A high surface area graphite was edge functionalized with hydroxyl groups (G-OH) through the reaction with KOH. G-CHO, with 4.5 mmol/g of functional group, was prepared from G-OH by means of the Reimer-Tiemann reaction. Characterization of the graphitic materials was performed with elemental analysis, titration, X-ray analysis, Raman spectroscopy and by estimating their Hansen solubility parameters. CS and G-CHO were mixed with mortar and pestle and carbon papers and aerogels were obtained from a stable acidic water suspension through casting and liophilization, respectively. Free standing and foldable carbon papers and monolithic aerogels based on a continuous covalent network between G-CHO and CS were prepared. G-CHO, which had about 22 stacked layers, was extensively exfoliated in the carbon paper, as confirmed by the absence of the 002 reflection of the graphitic crystallites in the XRD pattern. Carbon paper was found to be resistant to solvents and to be stable for $\text{pH} \geq 7$. Composites revealed electrical conductivity. The covalent network between the graphene layers and CS, suggested by the IR findings, accounts for these results. This work demonstrates the effectiveness of a continuous covalent network between chitosan and graphene layers edge functionalized with tailor made functional groups for the preparation of carbon papers and aerogels and paves the way for the scale up of such a type of composites.

Keywords

Chitosan, edge functionalized graphene layers, carbon papers, aerogels

Date received: 8 February 2021; revised: 11 April 2021; accepted: 23 April 2021

Introduction

Graphene (G)¹ has outstanding thermal,² mechanical² and electronic properties.³ A great amount of research is on graphene based nanocomposites,⁴ in order to bring to the macroscale the exceptional properties of graphene.

Bionanocomposites⁵ are an emerging class of materials, designed with the aim of achieving advanced structural and functional properties by using biobased polymers. As biopolymer, a great interest is for chitosan (CS), poly (*N*-acetyl-D-glucosamine), a copolymer of [1,4]-linked 2-acetamido-2-deoxy-D-glucopyranose and 2-amino-2-deoxy-D-glucopyranose.^{6,7}

Graphene and graphene related materials are increasingly used for the preparation of bionanocomposites.⁸ CS

presents several desirable properties such as non-toxicity, biodegradability, antimicrobial effect, and biocompatibility. Moreover, CS is used for its adsorption ability.^{9–15}

Department of Chemistry, Materials and Chemical Engineering “G. Natta,” Politecnico di Milano, Milan, Italy

Corresponding authors:

Vincenzina Barbera, Department of Chemistry, Materials and Chemical Engineering “G. Natta”, Politecnico di Milano, Via Mancinelli 7, Milan 20131, Italy.
Email: vincenzina.barbera@polimi.it

Maurizio Galimberti, Department of Chemistry, Materials and Chemical Engineering “G. Natta”, Politecnico di Milano, Via Mancinelli 7, Milan 20131, Italy.
Email: maurizio.galimberti@polimi.it



CS/G composites are used, in the biotechnological field, as nanocarrier for drug and gene delivery,¹⁶ for the growth and follow-up of primary cortical neuron cells,¹⁷ for the detection of human epidermal growth factor receptor.¹⁸ They are also used for preparing membranes with a lamellar structure for methanol dehydration,¹⁹ for the adsorption of substances such as tetracycline,²⁰ dyes,²¹ organic liquids,²² lead²³ and water contaminants,²⁴ for the catalytic reduction of oxygen in an iron and cobalt based system,²⁵ and for the preparation of high performance supercapacitors.²⁶

Among the CS/G nanocomposites, CS/G based hydrogels,²¹ aerogels,^{22,24,27,28} and carbon papers^{27,28} are the subject of increasing research activities. Aerogels²⁹ are indeed a unique class of materials with incredible lightness: typical average density is about 0.020 g/cm³. They have hierarchical porosities at the nanoscale and different shapes at the macroscale, such as: microspheres, powders, thin-film composites, monoliths. Carbon aerogels are attractive for a large variety of applications.^{30–32} There is a great interest for carbon papers, thanks to their mechanical properties³³ and to their ability to give rise to electrodes³⁴ and to stretchable supercapacitors,³⁵ to be used for biomimetics, electrocatalytic sensing and energy storage,³⁶ for structural composites³⁷ and chemical filters and membranes.³⁷

A key aspect for all the CS/G composites is the dispersion of the graphene layers and their interaction with the biopolymer. To achieve ultimate dispersion and interaction, in most cases a graphitic material is oxidized to graphene oxide (GO).³⁸ Chemical bonds can be established between CS and GO. Indeed, chitosan is presented as a tool to functionalize²⁴ and to crosslink the GO layers³⁹ and to establish covalent bonds with chemically converted graphene.⁴⁰ To have CS/G nanocomposites, GO is reduced^{18,19,25} to chemically reduced graphene oxide.⁴¹ For the oxidation-reduction cycle, dangerous and toxic chemicals and harsh reaction conditions are required and the transition metal (e.g. manganese from potassium permanganate) is hardly removed from the layers. Moreover, the bulk graphene structure is not completely restored: defective graphene layers are in the final composite.

It would be highly desirable to prepare graphene based aerogels and carbon papers with ultimate dispersion and integration of graphene layers with unperturbed structure, without performing the oxidation (to GO) – reduction cycle and without a troublesome modification of the graphene layers.

This was the aim of the research performed, in our group, over the last years. To this purpose, a simple and sustainable functionalization process was developed: *Janus* pyrrole compounds^{42–44} (PyC) were mixed and heated with the graphitic material. It was shown⁴⁴ that a domino reaction occurred, which led to the edge functionalization of the layers, whose bulk structure was substantially unaltered.^{42–45} Indeed, to have unperturbed graphene layers, the selective edge functionalization is a preferred approach.⁴⁶ Carbon papers and aerogels were prepared²⁸ with graphene layers

edge functionalized with 2-(2,5-dimethyl-1*H*-pyrrol-1-yl)propane-1,3-diol (SP), a PyC from serinol as the primary amine. The reported outcome²⁸ was the complete exfoliation of the graphitic aggregates, thanks to the synergy between the cation- π interaction of the cationic chitosan (from acidic solution) with the aromatic carbon substrate and the water compatibility of the graphene layers. Improvement of results was obtained with respect to the interaction of cationic chitosan with graphene layers without any functional group.²⁷ However, the edge located OH functional groups could not give rise to any chemical bond with CS. This is an issue for the composite material, in particular for the mechanical properties and the solvent resistance.

Hence, in the above commented prior art, there is not a report or a teaching on the preparation of a covalent network based on CS and graphene layers, with functionalization located only on the edges and unperturbed bulk structure. This work pursued the preparation of such an innovative network, through a simple and sustainable procedure: graphene layers with edge aldehydic functional groups able to chemically react with the amino groups of chitosan were used. As a first step, reaction was carried out between the layers and KOH/H₂O, introducing edge OH groups.⁴⁷ Functionalization with CHO groups was then obtained by performing the Reimer Tiemann reaction on the polyhydroxylated graphitic substrate. HSAG reaction with KOH was carried out at 0°C, with successive additions of CHCl₃: G-CHO was obtained.⁴⁷

Characterization of G-OH and G-CHO was carried out by means of Boehm titration, thermogravimetric analysis (TGA), Fourier-transformed infrared (FT-IR), and Raman spectroscopies. The Hansen solubility parameters (HSP)⁴⁸ and the Hansen sphere were estimated for G-OH and G-CHO, performing dispersion tests in solvents covering quite a broad range of solubility parameters.

CS/G-CHO composite materials were then prepared, with the aim of exploiting the reaction between aldehydic and amino groups. CS/G-CHO aerogel and paper were prepared by lyophilization and casting water suspensions, respectively. The research activity is summarized in Figure 1.

FT-IR and Raman spectroscopies and wide angle X-ray diffraction (WAXD) were used to characterize the CS/HSAG-CHO adducts. The thermal stability of the composites was checked by means of TGA, the solvent stability by using three classes of solvents and the direct electrical conductivity with the four-point probe method.

Methods

Reagents and solvents were commercially available and were used without further purification: KOH pellets (Carlo Erba Reagenti). Chitosan (high purity, Mw 110,000–150,000; degree of acetylation: ≤ 40 mol. %), acetic acid, methanol, glycol, 2-propanol, acetone, ethyl acetate, chloroform, xylene, toluene, hexane and

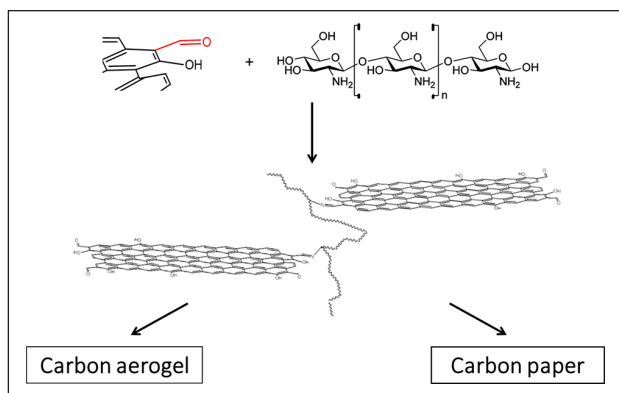


Figure 1. Summary of the research activity performed in this work.

dimethylformamide (DMF) (Aldrich). High surface area graphite (HSAG) was Synthetic Graphite 8427[®] (Asbury Graphite Mills Inc.), Characterization of HSAG has been reported by some of the authors in previous works.^{43,47,49,50} Analyzes have been performed on the samples used for the present work. Some of them are presented as Supplementary material, some others are discussed in the following.

The IR spectra were recorded in transmission mode (128 scan and 4 cm^{-1} resolution) using a ThermoElectron Continuum IR microscope coupled with a FTIR Nicolet Nexus spectrometer. For solid samples a small portion of the material was placed in a diamond anvil cell (DAC) and analyzed in transmission mode.

Raman spectra of powders and composites deposited on a glass slide were recorded with a Horiba Jobin Yvon Labram HR800 dispersive Raman spectrometer equipped with Olympus BX41 microscope and a 50X objective. The spectra were obtained as the average of four acquisitions (30 s for each acquisition) with a spectral resolution of 2 cm^{-1} . The Raman spectra reported in this work are the average of spectra recorded in five different points of the samples.

Wide angle X-ray diffraction (WAXD) patterns were obtained in reflection, with an automatic Bruker D8 Advance diffractometer, with nickel filtered $\text{Cu-K}\alpha$ radiation. Patterns were recorded in 0° – 90° as the 2θ range, being 2θ the peak diffraction angle. The D_{hkl} correlation length, in the direction perpendicular to the hkl crystal graphitic planes, and the distance between crystallographic planes have been calculated as reported by some of the authors in previous works.^{47,49}

Synthesis

Preparation of G-CHO by means of Reimer-Tiemann reaction performed on G-OH

Preparation and characterization of G-OH have been reported by some of the authors in previous works.^{47–49}

Characterization has been performed of the G-OH sample used for the present work and results are attached as supporting information.

Preparation and characterization of G-CHO have been reported by some of the authors in a previous work.⁴⁷ Characterization has been performed of the G-CHO sample used for the present work and results are discussed in the main text and attached as supporting information.

Preparation of G-CHO/chitosan nanocomposites

G-CHO/CS water suspensions. Chitosan (0.4 g) and G-CHO (0.4 g) were mixed for 5 min in a mortar with the help of a pestle. 8 mL of distilled water and four drops of an aqueous solution of acetic acid 99.7% (0.010 g , $9.9 \cdot 10^{-3}\text{ mol}$) were added. The so obtained suspension was sonicated for 15 min.

Chitosan carbon paper (G-CHO/CS paper). The water suspension obtained as reported in the previous paragraph was first sonicated for other 15 min and after poured on a glass plate in which an adhesive tape was used to delimit the area. Sheets were formed after water evaporation, at room temperature and atmospheric pressure (24 h).

Chitosan carbon aerogel (G-CHO/CS aerogel). The water suspension obtained as reported in the above paragraph was cooled to -30°C , then lyophilized (EDWARDS MODULO EF4-1596) under the following experimental conditions: $T = -50^\circ\text{C}$, $P = 5\text{ mbar}$, lyophilization time $t = 24\text{ h}$. G-CHO/CS aerogels with mass ratios equal to 1:1, 2:1 and 1:2 were obtained.

Characterization

Boehm titration of G-OH and G-CHO. Boehm titration was performed to quantitatively determine the content of oxygenated surface groups which were added after the functionalization procedures. The experimental procedure has been reported as the Supplementary material (S1).

Solubility parameters of G-CHO

Preparation of G-CHO dispersions in different solvents. Dispersions of G-CHO adducts were prepared at different concentrations: 1 mg/mL ; 0.5 mg/mL ; 0.3 mg/mL ; 0.1 mg/mL . Each dispersion was sonicated for 30 min using an ultrasonic bath (260 W). The dispersion (10 mL) of each sample was put in a Falcon[™] 15 mL Conical Centrifuge Tubes and centrifuged at 6000 rpm for 30 min. Evaluation of the dispersions' stability was qualitatively performed by putting a light at the back of the glass tubes, visually inspecting the dispersion after 3 days at rest. In this way, settling could be easily detected.

Calculation of the Hansen Solubility Sphere and Hansen Solubility Parameters

The calculation of the Hansen Solubility Parameters (HSP) for G-OH and G-CHO samples was performed applying the Hansen Solubility Sphere representation of miscibility. The detailed procedure for the determination of the Hansen solubility parameters have been reported as Supplementary material (S2).⁵¹

Characterization of G-CHO/chitosan nanocomposites. *UV-Vis spectroscopy* – G-CHO and G-CHO/CS suspensions (3 mL) were placed, by using a Pasteur pipette, in quartz cuvettes of 1 cm optical path (volume 1 or 3 mL) and analyzed by a spectrophotometer Hewlett Packard 8452A Diode Array Spectrophotometer. Pure water was used as blank for UV-Vis analysis. In the UV-visible spectrum, the absorption intensity was reported as a function of the wavelength of the radiation between 200 and 850 nm.

Conductivity measurements (four-point probe method) – Direct current (DC) electrical conductivity (s) was measured by the four point probe (FPP) method⁵² by using a hand applied FPP device (Jandel Engineering Ltd., UK) with a probe head with lineararrayed tungsten carbide needles (tip radii 300 μm , needles spacing 635 μm , loads 60 g) coupled with a Keithley 2601 electrometer. Data were acquired and analyzed by CSM/Win Semiconductor Analysis Program software (MDC, US).

Solvent resistance – Test was performed placing G-CHO/CS bio-nanocomposites (1 cm^2 , 50 nm thickness for the paper sample) in vials containing 2 mL of water, hexane and dimethyl formamide (DMF) respectively. Vials were left for 2 months to test the solvent stability.

Resistance in water at different pH. Test was performed placing G-CHO/CS bio-nanocomposites (1 cm^2 , 50 nm thickness for the paper sample) in vials containing 2 mL of water solutions at different pH. Vials were left for 2 months. Acids and bases used to tune pH were: HCl (38%), CH_3COOH (99.85%), NaHCO_3 , KOH.

Results

Preparation and characterization of graphene layers with oxygenated functional groups

The first step of the research was the preparation of graphene layers edge functionalized with $-\text{OH}$ and $-\text{CHO}$ groups. The latter functional group was the main objective of the activity, as it is suitable to react with the amino groups of chitosan. Preparation was performed by adopting the synthetic pathway already reported,⁴⁷ which is summarized in Figure SI-1.

Only main results are commented as follows, experimental findings are presented as supplementary material and some details are in the experimental part.

Pristine HSAG, washed with acetone, was characterized, in order to assess the substantial absence of oxygenated functional groups. Carbon content, determined via elemental analysis, was found to be 99.5%. TGA thermograph, FT-IR and Raman spectra are in Figures SI-2(a), SI-3(a), and SI-4(a) respectively. TGA analysis revealed no mass loss below 150°C and was about 2.3% up to 700°C. FT-IR spectrum did not show the presence of oxygenated functional groups and Raman spectrum revealed the relevant presence of the D band, as expected for a nanosized graphite from ball milling with pretty short lateral size.

Preparation and characterization of G-OH. To prepare G-OH, HSAG was reacted with KOH, with the help of thermal energy (details are in Sayyar et al.⁴⁰). In brief, the carbon allotrope and KOH powder were mixed (mass ratio=5/1) and kept at 100°C for 3 h. G-OH was isolated after careful washing, until neutral pH was achieved. G-OH sample was characterized by means of Boehm titration, a method able to detect the amount of acidic groups, TGA, FT-IR and Raman spectroscopies (details are in SI-4 and in Figures SI-2(b), SI-3(b) and SI-4(b)). Results of the characterizations are summarized as follows. From Boehm titration, the amount of functional groups was estimated to be 5.0 mmol/g (see Table SI-2). A mass loss larger than 12% was revealed by TGA between 150°C and 700°C and FT-IR spectrum showed the typical features of OH groups bonded to the graphene sheets. Raman spectra were very similar for HSAG and G-OH, with the enhancement, with respect to the HSAG spectrum, of D and D' peaks, as the only difference.

Preparation and characterization of G-CHO. The preparation of G-CHO was designed through the Reimer-Tiemann reaction of G-OH with CHCl_3 .⁴⁷ In brief, G-OH, KOH powder and H_2O were mixed at 0°C and CHCl_3 was added in three different steps, in small amounts. G-CHO, which contains OH and CHO groups, was obtained (see Figure SI-1). The characterization of G-CHO was carried out by means of Boehm titration, IR and Raman spectroscopies. The value obtained from the titration was of 4.5 mmol/g (Table SI-2). Such a value is very similar to the one (5.0 mmol/g) found in the case of G-OH and indicates that the reaction of G-OH with CHCl_3 does not lead to an appreciable modification of OH concentration, as it should be on the basis of the mechanism of the Reimer-Tiemann reaction: an equimolar amount of CHO and OH groups are expected on the graphene layers, as shown in Figure SI-1. FT-IR spectrum of G-CHO sample is reported in Figure SI-5, with a zoom in the 1800–700 cm^{-1} region in Figure SI-6. Details about the interpretation of the spectral features are in the literature.^{2,6} It is worth reporting here the following aspects, which are unique in G-CHO spectrum. At 1590 cm^{-1} the enhancement of the signal assigned to the E_{1u} IR active mode of the collective C=C stretching

vibration of graphitic materials, because of the chemical functionalization of the graphitic layers with OH and CHO groups. The presence of the strong band at 1220 cm^{-1} and of the broad and structured band at 1715 cm^{-1} which can be assigned to $\text{C}=\text{O}$ stretching vibration of aldehydic functionalities. Other bands at 1438 cm^{-1} , 1390 cm^{-1} , 1290 cm^{-1} , 1158 cm^{-1} , and 1100 cm^{-1} have a good correspondence with the absorptions of benzaldehyde and salicylaldehyde molecules. XRD analysis and Raman spectroscopy revealed that the Reimer-Tiemann reaction did not substantially alter the bulk structure of the graphitic material. The XRD pattern of G-CHO is shown in Figure 4(C)c and it will be discussed below in the text. In the Raman spectrum, new Raman components between G and D peaks, due to disordered sp^3 carbon structures, are not appreciable. The enhancement, with respect to the HSAG and G-OH spectra, of D and D' peaks can be observed, in line with the introduction of a further functional group.

Solubility parameters of HSAG, G-OH and G-CHO. The Hansen solubility parameters δ_D (dispersion), δ_p (polar), δ_H (hydrogen bonding), and the total solubility parameter δ_T were estimated for pristine HSAG, G-OH, and G-CHO. In brief, the graphitic material was suspended in solvents having different solubility parameters and the stability of the suspensions was inspected, as described in the experimental part. The Hansen solubility parameters of the solvents are in Table SI-3. The results of the inspection of dispersions' stability are qualitatively summarized in Table SI-4: good or bad mean, respectively that a homogenous dispersion was observed or that the adduct settled down. The functionalization of HSAG, with OH and with both OH and CHO, as the functional groups, led to the stability of the dispersions of the graphitic materials in a good number of solvents. Moving from these observations, the solubility parameters were estimated, by adopting the method described in the literature.^{43,51,53,54} Solubility spheres, which enclose the good solvents and exclude the bad ones, were generated.

Values of the solubility parameters and of the radius of the Hansen sphere for G-OH and G-CHO are in Table 1.

The spheres for G-OH and G-CHO are shown in Figure 2(a) and (b), respectively.

Stable dispersion of HSAG was obtained only in CHCl_3 and it was not possible to elaborate the Hansen sphere. The introduction of OH and CHO groups dramatically modified the solubility parameter of the graphene layers, which became dispersible in a good variety of solvents. The value of δ_T was found to be higher for G-OH. This finding could suggest an interaction between OH and CHO groups which could lead to a lower availability of the polar groups and hence to a less polar layers.

Both G-OH and G-CHO gave rise to stable water dispersions. UV-vis absorption analyzes on G-OH water dispersions have been already reported⁴⁷ and those on G-CHO are presented in this work as Supporting Information: the block diagram of the experimental procedure, the picture of water dispersions at different concentration, the UV-VIS spectra, with the relationship between the absorbance at 320 nm and the concentration of G-CHO in water, are shown in Figures SI-8 to SI-10 respectively. A linear correlation was found between G-CHO concentration (from 0.005 to 1 mg/mL) and the absorbance, taken immediately after the preparation of the dispersions. All the dispersions were observed to be stable at rest at least for 3 days and the UV absorption of the dispersion with 1 mg/mL as the concentration was the same even after centrifugation (3000 rpm , 30 min) (Figure SI-11).

Table 1. Hansen's solubility parameters and sphere radius for G-OH and G-CHO samples.

Sample	δ_D	δ_p	δ_H	Radius	δ_T^a
G-OH	15.7	14.8	16.1	16.3	26.9
G-CHO	11.2	13.5	13.4	13.6	22

Measure unit: $\text{MPa}^{1/2}$.
 $^a\delta_T^2 = (\delta_D^2 + \delta_p^2 + \delta_H^2)$.

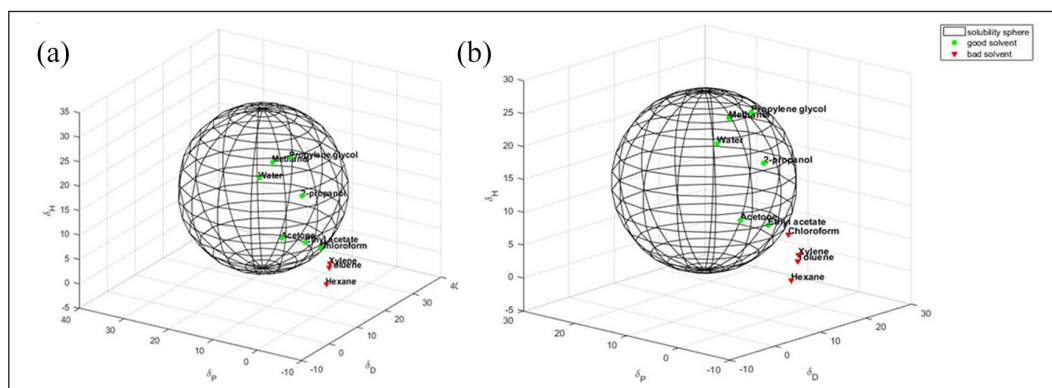


Figure 2. Hansen solubility sphere calculated for: (a) G-OH and (b) G-CHO. Hansen parameters ($\text{MPa}^{1/2}$): for G-OH: δ_D 15.7, δ_p 14.8 δ_H 16.1; for G-CHO: δ_D 11.2, δ_p 13.5 δ_H 13.4. The green circles correspond to the good solvents (within the radius of interaction), the red triangles to the bad solvents (outside the sphere).

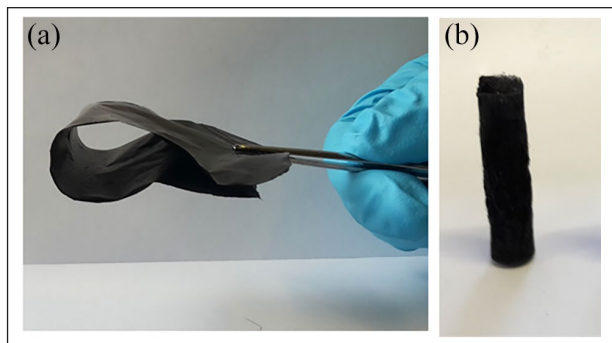


Figure 3. G-CHO/CS 1:1 free standing carbon paper (a) and monolithic aerogel (b).

Preparation of G-CHO/chitosan nanocomposites

Bionanocomposites were prepared, based on chitosan and G-CHO. Aim of the research was thus to covalently cross-link chitosan with the graphene layers, thanks to the reaction between the amino groups of chitosan and the aldehydic groups of G-CHO. The composites based on CS/G-CHO adducts were prepared as summarized in Figure SI-12 and described in the experimental part.

Preparation of CS/G-CHO water dispersions. First step was the preparation of CS/G-CHO water dispersions. In brief, G-CHO and CS were first premixed in a mortar with the help of a pestle. Dispersions were then prepared by introducing the CS/G-CHO mixture in a water solution of acetic acid. Different CS/G-CHO mass ratios were used: 1:1, 2:1, and 1:2.

The stability of water dispersions was tested for all the CS/G-CHO ratios prepared: they were observed to be stable for weeks. In Figure SI-13, are shown water dispersions of HSAG (Figure SI-13(a)), G-CHO (Figure SI-13(b)), CS/G-CHO with 1:1 as mass ratio and 1 mg/mL as CS/G-CHO concentration, after 1 month storage (Figure SI-13(c)) and after 30 min centrifugation at 6000 rpm (Figure SI-13(d)).

Preparation of CS/G-CHO carbon papers and aerogels. Carbon papers and aerogels were prepared moving from CS/G-CHO sonicated dispersions, having 2 mg/mL as CS/G-CHO concentration. For the preparation of carbon papers, CS/G-CHO dispersion was poured on a glass plate and water evaporation was allowed, whereas monolithic aerogels were obtained by freezing and lyophilizing the dispersion. In all cases flexible papers and monolithic aerogels were obtained.

Free-standing CS/G-CHO 1:1 paper, with a thickness of 36 μm , and monolithic aerogel are shown in Figure 3.

As it can be seen in Figure 3, the CS/G-CHO paper (1:1) was flexible and perfectly foldable, reaching a curvature radius close to 180° (see Figure SI-14) without the appearance of cracks.

Analytical characterization of CS/G-CHO carbon papers and aerogels. FT-IR spectra of chitosan, CS/G-CHO paper and aerogel (1:1) and G-CHO are reported in Figure 4, in the full 4000–700 cm^{-1} region in Figure 4(A) and with a zoom in the region 1800–700 cm^{-1} in Figure 4(B).

The spectrum of pure chitosan (Figure 4(A)d and (B)d) shows signals characteristic of chitin and deacetylated chitin units. Peaks located at 3477 cm^{-1} , 3444 cm^{-1} , 3268 cm^{-1} , and 3107 cm^{-1} , are assigned to the stretching vibrations of –OH, –NH-R, and –NH₂ groups of chitosan, respectively. Bands at 1659 cm^{-1} and 1625 cm^{-1} has been assigned to the –C=O stretching vibrations (amide I) of the amide group –C=ONHCH₃, typical for crystalline α -chitin.⁵⁵ The sharp peak at 1378 cm^{-1} is assigned to the symmetric bending of methyl groups (“umbrella” motion of chitin groups).

In the spectra of the CS/G-CHO paper (Figure 4(A)b and (B)b) and aerogel (Figure 4(A)c and (B)c) the G_{IR} peak at 1590 cm^{-1} (the reflection due to C=C conjugation in graphitic materials) and the main absorptions of CS can be observed. However, all the absorption bands are broader: there is a peak shift and band overlapping. This observation supports the occurrence of structural disorder for the CS moiety in the carbon paper. The band at 1715 cm^{-1} (assigned to –C=O stretching vibration) is reduced in intensity and a new medium-weak feature at 1656 cm^{-1} appears. In this region features due to amidic functionalities of CS are expected. These findings, already reported in the preliminary investigation on the adducts made by CS and G-CHO,⁴⁷ appear as the indication of the formation of the amidic group from the reaction of the amino groups of chitosan and the CHO substituent on the graphene layers.

Organization at the solid state of CS/G-CHO composites was investigated by means of WAXD analysis. Figure 4(C) shows WAXD patterns of pristine HSAG (Figure 4(C)a), G-CHO (Figure 4(C)b), chitosan powder (Figure 4(C)c), chitosan treated with acetic acid (Figure 4(C)d), CS/G-CHO 1:1 aerogel (Figure 4(C)e) and paper (Figure 4(C)f).

The peaks at 26.6° as 2 θ value in Figure 4(C)a and in (C)b are due to the (002) reflection of HSAG and G-CHO, respectively. The correlation length of the crystallites was calculated by applying the Scherrer equation (see experimental section and the supplementary material) and the number of stacked layers was estimated to be about 35 and 22 for HSAG and G-CHO, respectively. 100 and 110 reflections indicate the in plane crystalline organization. The correlation length for the 110 crystallites was estimated to be in a range from 26.5 nm to 28 nm. These findings suggest that the in plane order is not substantially altered passing from HSAG to G-CHO. The crystallinity of chitosan is demonstrated by two reflections at 10.2° and 19.9° as 2 θ angles in Figure 4(C)f.

The patterns in Figure 4(C)c and (C)d suggest that in both aerogel and paper there was a substantial modification of the solid state organization of both chitosan and

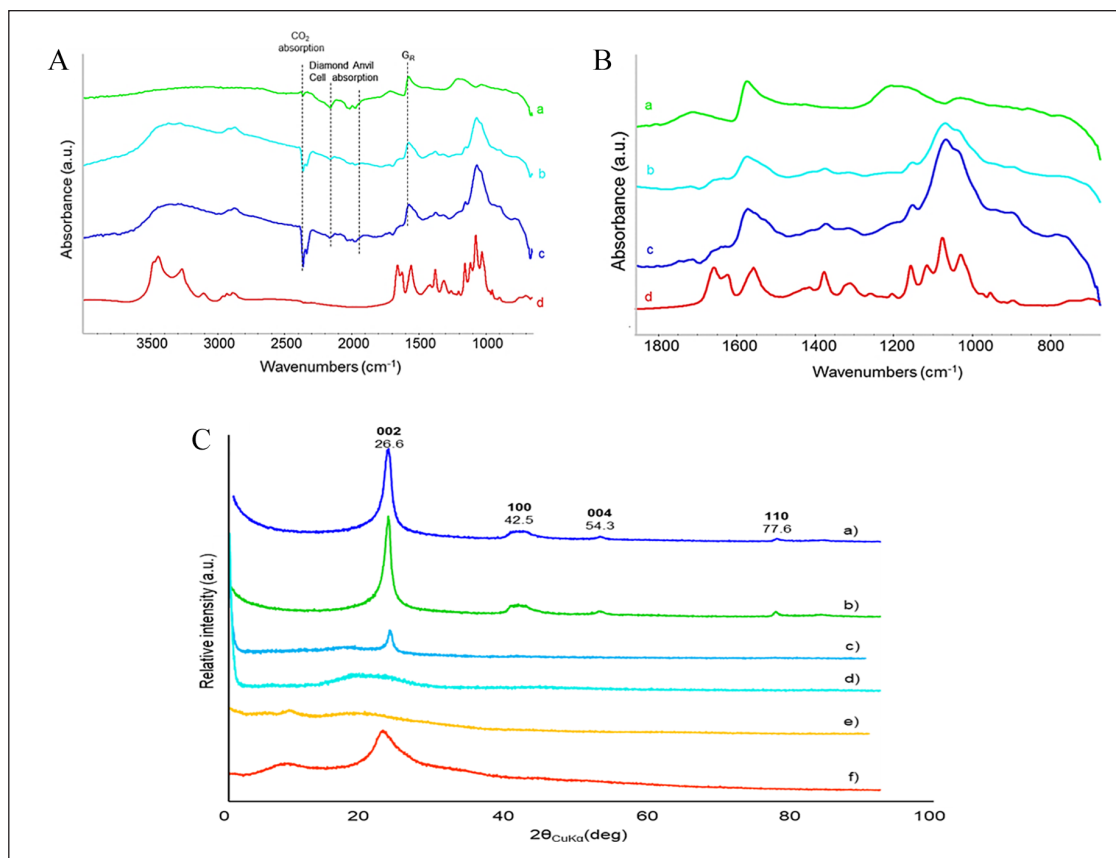


Figure 4. FT-IR spectra of G-CHO (a), CS/G-CHO 1:1 paper (b), CS/G-CHO 1:1 aerogel (c), and chitosan (d): in the full region 4000–700 cm^{-1} (A) and zoom in the region 1800–700 cm^{-1} (B); (C) WAXD patterns of pristine HSAG (a), G-CHO (b), CS/G-CHO 1:1 aerogel (c), CS/G-CHO 1:1 paper (d), CS film in acetic acid (e), and chitosan powder (f).

G-CHO. In the WAXD pattern of the CS/G-CHO aerogel (Figure 4(C)c) the (002) reflection of G-CHO is visible. Reduction of correlation length of (002) crystallites was found and the number of stacked layers was estimated to be about 10, but the complete exfoliation of the graphitic aggregates did not occur. Instead, in the WAXD pattern of the paper based on CS/G-CHO (Figure 4(C)d), the (002) reflection is absent and signals of chitosan crystals are not detectable. In order to understand the changes of crystallinity observed for chitosan in CS/G-CHO aerogel and paper, CS was treated with acetic acid, in the absence of G-CHO, and the isolated film was analyzed by WAXD. The pattern is shown in Figure 4(C)e and reveals broad crystalline peaks at 20.5° and 11.8° as 2θ value. Compared with the chitosan powder peaks, they are less resolved and also slightly displaced. It appears that the process of casting a chitosan film from an acetic acid solution allows some crystallization upon drying, while the presence of G-CHO inhibits the crystallization.

Resistance to solvents and in a range of pH. The resistance to solvents of CS/G-CHO papers and aerogels, with 1:1, 2:1 and 1:2 as CS/G-CHO ratios, was investigated, by using

solvents such as DMF, H_2O and n-hexane, in a wide range of values as solubility parameters (δ_T : $\text{H}_2\text{O}=30.1$, DMF=24.8, hexane=14.9). Vials containing specimens of the paper and aerogels kept for two days in the solvents are shown in Figure SI-15. The mass of the samples, before and after the storage, are in Tables SI-4 to SI-6.

Carbon papers were observed to be stable in all the solvents, with a very small solvent absorption, at all the CS/G-CHO ratios. Aerogels revealed a clearly detectable absorption in DMF, at all the CS/G-CHO ratios. In water as the solvent, the nanocomposite swelled and loosed its integrity. In hexane, stability of the nanocomposite was observed at 1:1 and 2:1 as the G-CHO/CS ratios, whereas solvent absorption was clearly detected at 1:2 as G-CHO/CS ratio.

The pH resistance of CS/G-CHO paper and aerogel in water at different pH was investigated, by using HCl, CH_3COOH , NaHCO_3 and KOH to modulate the pH. Suspensions of the nanocomposites were visually inspected (see Figure SI-16). Nanocomposites taken from the suspensions were weighed. The mass of the CS/G-CHO nanocomposites, at 1:1, 2:1 and 1:2 ratios, before and after the storage, are in Tables SI-7 to SI-9, respectively.

Table 2. DC conductivity of CS/G-CHO papers with different graphite content.

CS/G-CHO ratio ^a	σ (S/m)
Chitosan	1E ⁻⁸
1:1	0.013
1:2	0.10
2:1	0.012

^aContent respect to 100mg of chitosan.

Both carbon papers and aerogels were stable, at all the G-CHO/CS ratios, at pH \geq 7, whereas the samples loosed their integrity at pH = 1 and 4.

Electrical conductivity of CS/G-CHO papers was measured by the four-point probe method.⁵² In Table 2 are reported the measured values of room temperature DC conductivity for composites with different CS/G-CHO ratios.

For carbon papers, a critical value of CS/G-CHO ratio has to be overcome in order to obtain values of electrical conductivity in line with those reported in the literature. At G-CHO/CS ratio of at least 1:1 sufficient values of conductivity for many electrical applications are reached.⁵⁶

Discussion

G-OH and G-CHO as building block for chitosan based nanocomposites

Graphene, with its very high surface area and outstanding thermal and electrical conductivities, can really give rise to high performance nanocomposites, such as carbon papers and aerogels. However, to achieve that, mandatory is to preserve the structure of the graphene layers and to obtain their ultimate integration in the composite matrix. The edge functionalization of graphene layers is a successful road for achieving such objectives, particularly if the edges can be decorated with tailor made functional groups, able even to chemically react with the matrix. The preparation of G-OH and G-CHO appears to be a successful example, for preparing composites based on chitosan.

It has been already reported^{49,56} that the edge functionalization of graphene layers with hydroxyl anions, to form G-OH, occurs through a nucleophilic attack followed by re-aromatization, which is the real driving force of the process. This reaction leads to the introduction of a remarkable amount of OH functional groups, as detected by means of Boehm titration, which could be ascribed to the large surface area of HSAG (330 m²/g).

The controlled reaction (at 0°C with successive additions of the reagent) of the polyhydroxylated layers with CHCl₃ promotes the functionalization with aldehydic groups, in ortho position with respect to the OH groups. The value of 4.5 mmol/g (Table SI-2), obtained from the Boehm titration, is consistent with the reaction mechanism: indeed, the

Reimer-Tiemann reaction leads to the formation of 1 CHO mole and three KCl moles for each OH mole. As reported above in the Discussion, the G-OH used was found to have 5 mmol/g of OH groups (Table SI-2).

The bulk structure of the layers is substantially unaffected by the functionalization process. This is indicated by both XRD pattern and Raman spectrum. Both in the case of G-OH and G-CHO, the in plane order revealed by XRD peaks remains substantially unaffected and the enhancement of D and D' peaks in the Raman spectrum is compatible with the introduction of functional groups.

The solubility parameter of the layers were dramatically modified by the introduction of the edge functional groups. The graphitic layers with OH and OH/CHO functional groups are compatible with polar solvents and polar matrices. It is interesting to observe that the value of δ_T decreased from G-OH to G-CHO, from 26.9 to 22 and also the value of the radius, from 16.3 to 13.6. This finding could be seen as unexpected: larger amount of polar functional groups should lead to a larger δ_T value and, in particular, to a larger δ_p value. An explanation could be based on the interaction between vicinal OH and CHO groups, through an intramolecular hydrogen bonding. Results from IR investigation support this hypothesis: the well-defined band at 1715 cm⁻¹ observed in the spectrum of G-CHO and assigned to -C=O stretching vibration of aldehydic functionalities is typical of salicylic aldehyde like compounds, which are characterized by the intramolecular bonds.

This paper strengthens the results already published⁴⁷ on G-OH and G-CHO, gives a demonstration of the robustness of the functionalization technique, based on a complete characterization of the functionalized graphitic products and shows that the Reimer-Tiemann reaction on polyhydroxylated graphene layers is a suitable tool for the preparation of nanocomposites, based on graphene and chitosan.

CS/G-CHO nanocomposites

The experimental procedure for the preparation of carbon papers and aerogels appears to be simple, easily reproducible. The mechanical energy to promote the interaction between CS and G-CHO (as indicated in the scheme in Figure SI-12) was achieved by simply using mortar and pestle. The stability of G-CHO water dispersion and the use of cationic CS, easily soluble in water, can be considered to play a key role. Definitely, cationic CS favorably interacts with aromatic substrates such as the graphene layers, as already demonstrated.^{27,28} However, the key aspect of this work is the establishment of a covalent bond between the layer and CS, thanks to the reaction between the amino and the CHO groups. It can be thus summarized that preparation of bionanocomposites was performed in an acidic media in order to: (i) protonate the amines and to induce the cation- π interaction between the polymer and

the graphene layers; (ii) catalyze the condensation reaction between the amine and the carbonyl and induce the formation of the imine functional group. Indications for the formation of the imine bond can be drawn from IR spectra, both of carbon papers and aerogels.

As mentioned above, water dispersions of CS/G-CHO adducts were stable, for days at rest, and could be thus considered as suitable starting material for the preparation of CS/G-CHO nanocomposites.

However, it is worth focusing the attention on the consequences on the composites properties of a graphene/chitosan network based on covalent bonds.

Findings indeed interesting arise from XRD results. In the pattern of the CS/G-CHO carbon paper the (002) reflection of stacked graphene layers is not visible. In a recent paper by some of the authors,²⁸ exfoliation of HSAG to few layers graphene⁵⁷ was obtained in CS based carbon papers and aerogels, but the (002) reflection was absent only in the XRD pattern of the aerogel swollen in water. It is widely acknowledged that the absence of an evidence is not the evidence of an absence. However, the pattern in Figure 4(C)e allows to comment that extensive HSAG exfoliation, down to few layers graphene and even graphene, can occur by simply preparing the carbon paper. To achieve this result, the formation of covalent bonds between CS and the graphene layers is definitely beneficial. To the best of our knowledge, for the first time, extensive (if not complete) exfoliation of a graphitic aggregate was obtained in a carbon paper by simply mixing CS and a nanosized graphite, casting then the water dispersion.

Carbon papers were found to be stable in solvents in a wide range of solubility parameters and at all the G-CHO/CS ratios and to $\text{pH} \geq 7$. Aerogels were analogously stable in the same pH range but revealed the ability to absorb the solvents, up to the crumbling of the sample in water. The porosity of the aerogels appears to be responsible for this behavior. Interestingly, also the aerogels with 2:1 as the G-CHO/CS ratio were stable in hexane. These results suggest the key role of the crosslinking of chitosan with the graphene layers. Indeed, the behavior at $\text{pH} = 1$ and 4 can be attributed to the hydrolysis of the imino bond.

The key aspect of this work appears to be the formation of the imino bond between G-CHO and chitosan. The nucleophilic carbonyl addition reaction of the amine to the aldehyde is favored by the acidic medium and by the donation of energy (sonication process). Reaction of chitosan with aldehydes are well documented in the literature.⁵⁸ Indeed, chitosan is crosslinked with glutaraldehyde. To demonstrate the easy reactivity of the repeating unit of chitosan with an aromatic aldehyde, in this work the synthesis of 6-(hydroxymethyl)-3-(4-methoxybenzylideneamino)tetrahydro-2H-pyran-2,4,5-triol from glucosamine and 4-methoxybenzaldehyde was performed, in the same reaction conditions used for for bionanocomposites, hence at nominal room temperature. The reaction pathway of the model reaction is reported in Figure SI-17. The reaction

occurred only by mixing the aldehyde, the amine and acetic acid and giving sonication energy.¹ ¹H NMR spectrum, consistent with the structure of the hypothesized product is reported in Figure SI-18.

Electrical conductivity was found in CS/G-CHO nanocomposites. This property could be tuned, not only by selecting a proper graphite grade, but also through the chemical composition of the composite. As a perspective, it would be interesting to investigate the thermal conductivity of CS/G-CHO materials: the continuous network based on covalent bonds could be indeed beneficial.

Conclusions

Carbon papers and aerogels were simply created by first mixing, with mortar and pestle, chitosan and graphene layers edge functionalized with aldehydic groups, then casting or liophilizing stable water dispersions of CS/G-CHO adducts. Such a simple procedure led to the formation of free standing and foldable papers and monolithic aerogels, to the extensive exfoliation of graphene layers, to great stability to solvents and pH. All these results are convincingly explained by the existence of a continuous covalent network between CS and the graphene layers. It would be desirable to scale up the preparation of the nanocomposites presented in this paper. However, the reaction of nanographite with KOH and the successive Reimer-Tiemann reaction have been so far explored at the lab scale. This could be seen as a limitation of the research here reported.

Acknowledgements

Authors gratefully acknowledge Dr. Luigi Brambilla (Politecnico di Milano) for FT-IR and Raman spectra.

Contributorship

Conceptualization, V.B. and M.G.; methodology, V.B. and M.G.; validation, G.T.; formal analysis, V.B. and G.T.; synthesis and characterization, V.B. and G.T.; data curation, V.B. and G.T.; writing – original draft preparation, V.B. and M.G.; writing – review and editing, V.B. and M.G.; supervision, M.G. and V.B.; project administration, M.G. and V.B. All authors have read and agreed to the published version of the manuscript.

Declaration of Conflicting Interests

The author(s) declared no potential conflicts of interest with respect to the research, authorship, and/or publication of this article.

Funding

The author(s) received no financial support for the research, authorship, and/or publication of this article.

ORCID iD

Vincenzina Barbera  <https://orcid.org/0000-0002-4503-4250>

Supplemental material

Supplemental material for this article is available online.

References

- Kostarelos K and Novoselov KS. Graphene devices for life. *Nat Nanotechnol* 2014; 9(10): 744.
- Kumar A, Sharma K and Dixit AR. A review of the mechanical and thermal properties of graphene and its hybrid polymer nanocomposites for structural applications. *J Mater Sci* 2019; 54(8): 5992–6026.
- Novoselov KS, Morozov SV, Mohinddin TMG, et al. Electronic properties of graphene. *Phys Status Solidi (b)* 2007; 244(11): 4106–4111.
- Young RJ, Kinloch IA, Gong L and Novoselov KS. The mechanics of graphene nanocomposites: a review. *Compos Sci Technol* 2012; 72(12): 1459–1476.
- Darder M, Aranda P and Ruiz-Hitzky E. Bionanocomposites: a new concept of ecological, bioinspired, and functional hybrid materials. *Adv Mater* 2007; 19(10): 1309–1319.
- Rinaudo M. Chitin and chitosan: properties and applications. *Prog Polym Sci* 2006; 31(7): 603–632.
- Jianguo L, Yanqun L, Haiyan L, et al. Preparation, bioactivity and mechanism of nano-hydroxyapatite/sodium alginate/chitosan bone repair material. *J Appl Biomater Funct Mater* 2018; 16(1): 28–35.
- Wang Y, Li Z, Wang J, Li J and Lin Y. Graphene and graphene oxide: biofunctionalization and applications in biotechnology. *Trends Biotechnol* 2011; 29(5): 205–212.
- Jawad AH, Abdulhameed AS, Abd Malek NN and Alothman ZA. Statistical optimization and modeling for color removal and COD reduction of reactive blue 19 dye by mesoporous chitosan-epichlorohydrin/kaolin clay composite. *Int J Biol Macromol* 2020; 164: 4218–4230.
- Jawad AH, Mubarak NSA and Abdulhameed AS. Hybrid crosslinked chitosan-epichlorohydrin/TiO₂ nanocomposite for reactive red 120 dye adsorption: kinetic, isotherm, thermodynamic, and mechanism study. *J Polym Environ* 2020; 28(2): 624–637.
- Abd Malek NN, Jawad AH, Abdulhameed AS, Ismail K and Hameed BH. New magnetic Schiff's base-chitosan-glyoxal/fly ash/Fe₃O₄ biocomposite for the removal of anionic azo dye: an optimized process. *Int J Biol Macromol* 2020; 146: 530–539.
- Reghioua A, Barkat D, Jawad AH, Abdulhameed AS and Khan MR. Synthesis of Schiff's base magnetic crosslinked chitosan-glyoxal/ZnO/Fe₃O₄ nanoparticles for enhanced adsorption of organic dye: modeling and mechanism study. *Sustain Chem Pharm* 2021; 20: 100379.
- Jawad AH, Abdulhameed AS, Surip SN and Sabar S. Adsorptive performance of carbon modified chitosan biopolymer for cationic dye removal: kinetic, isotherm, thermodynamic, and mechanism study. *Int J Environ Anal Chem*. Epub ahead of print 27 August 2020. DOI: 10.1080/03067319.2020.1807966.
- Jawad AH, Abdulhameed AS and Mastuli MS. Mesoporous crosslinked chitosan-activated charcoal composite for the removal of thionine cationic dye: comprehensive adsorption and mechanism study. *J Polym Environ* 2020; 28(3): 1095–1105.
- Jawad AH, Mubarak NSA and Abdulhameed AS. Tunable Schiff's base-cross-linked chitosan composite for the removal of reactive red 120 dye: adsorption and mechanism study. *Int J Biol Macromol* 2020; 142: 732–741.
- Bao H, Pan Y, Ping Y, et al. Chitosan-functionalized graphene oxide as a nanocarrier for drug and gene delivery. *Small* 2011; 7(11): 1569–1578.
- Meng S and Peng R. Growth and follow-up of primary cortical neuron cells on non functionalized graphene nanosheet film. *J Appl Biomater Funct Mater* 2016; 14(1): e26–e34.
- Tabasi A, Noorbakhsh A and Sharifi E. Reduced graphene oxide-chitosan-aptamer interface as new platform for ultrasensitive detection of human epidermal growth factor receptor 2. *Biosens Bioelectron* 2017; 95: 117–123.
- Hung WS, Chang SM, Lecaros RLG, et al. Fabrication of hydrothermally reduced graphene oxide/chitosan composite membranes with a lamellar structure on methanol dehydration. *Carbon* 2017; 117: 112–119.
- Huang B, Liu Y, Li B, et al. Effect of Cu (II) ions on the enhancement of tetracycline adsorption by Fe₃O₄@ SiO₂-chitosan/graphene oxide nanocomposite. *Carbohydr Polym* 2017; 157: 576–585.
- Omidi S and Kakanejadifard A. Eco-friendly synthesis of graphene-chitosan composite hydrogel as efficient adsorbent for Congo red. *RSC Adv* 2018; 8(22): 12179–12189.
- Li J, Meng H, Xie S, Zhang B, Li L and Yu M. Ultra-light, compressible and fire-resistant graphene aerogel as a highly efficient and recyclable adsorbent for organic liquids. *J Mater Chem A* 2014; 2(9): 2934–2941.
- Medina RP, Nades ET, Ballesteros FC and Rodrigues DF. Incorporation of graphene oxide into a chitosan-poly (acrylic acid) porous polymer nanocomposite for enhanced lead adsorption. *Environ Sci Nano* 2016; 3(3): 638–646.
- Kumar ASK and Jiang SJ. Chitosan-functionalized graphene oxide: a novel adsorbent for efficient adsorption of arsenic from aqueous solution. *J Environ Chem Eng* 2016; 4(2): 1698–1713.
- Aghabarari B, Nezafati N, Roca-Ayats M, Capel-Sánchez MC, Lázaro MJ and Martínez-Huerta MV. Effect of molybdophosphoric acid in iron and cobalt graphene/chitosan composites for oxygen reduction reaction. *Int J Hydrog Energy* 2017; 42(46): 28093–28101.
- Sun G, Li B, Ran J, Shen X and Tong H. Three-dimensional hierarchical porous carbon/graphene composites derived from graphene oxide-chitosan hydrogels for high performance supercapacitors. *Electrochim Acta* 2015; 171: 13–22.
- Barbera V, Guerra S, Brambilla L, et al. Carbon papers and aerogels based on graphene layers and chitosan: direct preparation from high surface area graphite. *Biomacromolecules* 2017; 18(12): 3978–3991.
- Guerra S, Barbera V, Vitale A, et al. Edge functionalized graphene layers for (ultra) high exfoliation in carbon papers and aerogels in the presence of chitosan. *Materials* 2020; 13: 39.
- Kistler SS. Coherent expanded aerogels and jellies. *Nature* 1931; 127: 741.
- Haji S and Erkey C. Removal of dibenzothiophene from model diesel by adsorption on carbon aerogels for fuel cell applications. *Ind Eng Chem Res* 2003; 42(26): 6933–6937.

31. Biener J, Stadermann M, Suss M, et al. Advanced carbon aerogels for energy applications. *Energy Environ Sci* 2011; 4(3): 656–667.
32. Moreno-Castilla C and Maldonado-Hódar FJ. Carbon aerogels for catalysis applications: an overview. *Carbon* 2005; 43(3): 455–465.
33. Liu Y, Xie B, Zhang Z, Zheng Q and Xu Z. Mechanical properties of graphene papers. *J Mech Phys Solids* 2012; 60(4): 591–605.
34. Huang X, Zeng Z, Fan Z, Liu J and Zhang H. Graphene-based electrodes. *Adv Mater* 2012; 24(45): 5979–6004.
35. Zang J, Cao C, Feng Y, Liu J and Zhao X. Stretchable and high-performance supercapacitors with crumpled graphene papers. *Sci Rep* 2014; 4(1): 1–7.
36. Zhang M, Hou C, Halder A, Wang H and Chi Q. Graphene papers: smart architecture and specific functionalization for biomimetics, electrocatalytic sensing and energy storage. *Mater Chem Front* 2017; 1(1): 37–60.
37. Yagoh H, Murayama H, Suzuki T, Tominaga Y, Shibuya N and Masuda Y. Simultaneous monitoring method of polycyclic aromatic hydrocarbons and persistent organic pollutants in the atmosphere using activated carbon fiber filter paper. *Anal Sci* 2006; 22(4): 583–590.
38. Dreyer DR, Ruoff RS, Bielawski CW, Dreyer DR, Ruoff RS and Bielawski CW. From conception to realization: an historical account of graphene and some perspectives for its future. *Angew Chem Int Ed Engl* 2010; 49: 9336–9344.
39. de Luna MS, Ascione C, Santillo C, et al. Optimization of dye adsorption capacity and mechanical strength of chitosan aerogels through crosslinking strategy and graphene oxide addition. *Carbohydr Polym* 2019; 211: 195–203.
40. Sayyar S, Murray E, Gambhir S, Spinks G, Wallace GG and Officer DL. Synthesis and characterization of covalently linked graphene/chitosan composites. *JOM* 2016; 68(1): 384–390.
41. Mauro M, Cipolletti V, Galimberti M, Longo P and Guerra G. Chemically reduced graphite oxide with improved shape anisotropy. *J Phys Chem C* 2012; 116: 24809–24813.
42. Galimberti M, Barbera V, Guerra S, et al. Biobased Janus molecule for the facile preparation of water solutions of few layer graphene sheets. *RSC Adv* 2015; 5(99): 81142–81152.
43. Barbera V, Bernardi A, Palazzolo A, Rosengart A, Brambilla L and Galimberti M. Facile and sustainable functionalization of graphene layers with pyrrole compounds. *Pure Appl Chem* 2018; 90(2): 253–270.
44. Barbera V, Brambilla L, Milani A, et al. Domino reaction for the sustainable functionalization of few-layer graphene. *Nanomaterials* 2019; 9(1): 44.
45. Galimberti M, Barbera V, Guerra S and Bernardi A. Facile functionalization of sp² carbon allotropes with a biobased Janus molecule. *Rubber Chem Technol* 2017; 90(2): 285–307.
46. Sun Z, Kohama SI, Zhang Z, Lomeda JR and Tour JM. Soluble graphene through edge-selective functionalization. *Nano Res* 2010; 3(2): 117–125.
47. Barbera V, Brambilla L, Porta A, et al. Selective edge functionalization of graphene layers with oxygenated groups by means of Reimer-Tiemann and domino Reimer-Tiemann/Cannizzaro reactions. *J Mater Chem A* 2018; 6(17): 7749–7761.
48. Hansen CM. *Hansen solubility parameters: a user's handbook*. 2nd ed. Boca Raton, FL: CRC Press, 2007.
49. Barbera V, Porta A, Brambilla L, et al. Polyhydroxylated few layer graphene for the preparation of flexible conductive carbon paper. *RSC Adv* 2016; 6(90): 87767–87777.
50. Musto S, Barbera V, Cipolletti V, Citterio A and Galimberti M. Master curves for the sulphur assisted crosslinking reaction of natural rubber in the presence of nano- and nanostructured sp² carbon allotropes. *EXPRESS Polym Lett* 2017; 11(6): 435–448.
51. Locatelli D, Barbera V, Brambilla L, Castiglioni C, Sironi A and Galimberti M. Tuning the solubility parameters of carbon nanotubes by means of their adducts with Janus pyrrole compounds. *Nanomaterials* 2020; 10(6): 1176.
52. Swartzendruber LJ. Four-point probe measurement of non-uniformities in semiconductor sheet resistivity. *Solid State Electron* 1964; 7: 413–422.
53. Olynick DL, Ashby PD, Lewis MD, et al. The link between nanoscale feature development in a negative resist and the Hansen solubility sphere. *J Polym Sci B Polym Phys* 2009; 47(21): 2091–2105.
54. Hansen CM and Beerbower A. Solubility parameters. *Kirk-Othmer Encycl Chem Technol* 1971; 2(2): 889–910.
55. Brugnerotto J, Lizardi J, Goycoolea FM, Argüelles-Monal W, Desbrieres J and Rinaudo M. An infrared investigation in relation with chitin and chitosan characterization. *Polymer* 2001; 42(8): 3569–3580.
56. Zhan Y, Lavorgna M, Buonocore G and Xia H. Enhancing electrical conductivity of rubber composites by constructing interconnected network of self-assembled graphene with latex mixing. *J Mater Chem* 2012; 22(21): 10464–10468.
57. Kauling AP, Seefeldt AT, Pisoni DP, et al. The worldwide graphene flake production. *Adv Mater* 2018; 30(44): 1803784.
58. Azevedo EPD. *Aldehyde-functionalized chitosan and cellulose: chitosan composites: application as drug carriers and vascular bypass grafts* [PhD dissertation]. Iowa City: University of Iowa, 2011. DOI: 10.17077/etd.3zsb1awf.